

# INSIGHT INTO THE DEGRADATION MECHANISM OF F-53B, THE ALTERNATIVE TO PFOS AS CHROME MIST SUPPRESSANT IN CHINA, BY UV/SULFITE PROCESS

Bao YX, Huang J\*

State Key Joint Laboratory of Environment Simulation and Pollution Control (SKJLESPC), Beijing Key Laboratory for Emerging Organic Contaminants Control (BKLEOC), School of Environment, POPs Research Center, Tsinghua University, Beijing, China, 100084, [baoja2008@163.com](mailto:baoja2008@163.com); [\\*huangjun@mail.tsinghua.edu.cn](mailto:*huangjun@mail.tsinghua.edu.cn)

## Introduction

Chrome mist suppressant (CMS) is one of the major exempted uses for PFOS in China until now. Yet, this exemption will be ended in 2019. Monochlorinated-polyfluorinated-ether sulfonate (F-53B,  $\text{ClC}_8\text{F}_{16}\text{O}_4\text{S}\cdot\text{K}$ ) has been used for almost 40 years in CMS formulations, it was estimated have been emitted into environment 10-14 t/y during 2006-2015<sup>1</sup>. F-53B has been found to be still toxic<sup>2</sup>, and stronger bio-accumulation/persistence<sup>3,4</sup> relative to PFOS. Despite many adverse effects reported, considering the importance for an effective CMS in the electroplating industry and uncertainties of the use of non-fluorinated CMS, it is likely that the production of F-53B will continue to increase after the phase-out of PFOS in China<sup>5</sup>. Until now, only adsorption was reported to be effective to remove F-53B from water<sup>6</sup>, and it is not oxidizable by heat activated persulfate<sup>7</sup>. Consequently, it would lead to great threats to ecosystem health. In this study, we investigated the degradation mechanism of F-53B in water for the first time, and the far much better degradability of F-53B vs. PFOS in strong reductive system (UV/sulfite, which can generate strong reductant aqueous electron:  $e_{\text{aq}}^-$ ,  $E = -2.9$  V) was illustrated. Furthermore, the trace amount of F-53B (initial concentration: 65.7  $\mu\text{g/L}$ ) was successfully eliminated from real electroplating effluent.

## Materials and methods

F-53B (CAS no.: 73606-19-6, >96%) and F-53 (CAS no.: 68136-88-9, >96%) were obtained from the Shanghai Institute of Organic Chemistry, Chinese Academy of Sciences. PFOS (CAS no.: 2795-39-3, >98%) was provided by TCI, Japan. PFOS, F-53 and F-53B were dissolved in ultrapure water to 0.16 mM. Photochemical reactions were conducted in quartz tubes (45 mL) on a turnplate with 10 rpm in the reactor (RPR200, Southern New England Ultraviolet (Rayonet) Co., USA), surrounded by 16 lamps (with 253.7 nm wavelength). The PFOS, F-53 and F-53B were analyzed using high performance liquid chromatography (LC-20AT) with conductivity detector (CDD-10A vp) from Shimadzu, Japan. Degradation intermediates were quantified using LC/MS/MS, ((DIONEX UltiMate 3000, USA) with a tandem two-stage mass spectrometer (MS/MS, API 3200, AB SCIEX, USA). Density functional theory calculations on PFOS, F-53, F-53B and other molecules were conducted on the Gaussian 09.

## Results and discussion:

**Degradation kinetics in pure water:** F-53B could be easily decomposed by attack of  $e_{\text{aq}}^-$ , more than 99% of Cl was recovered once F-53B was not detectable (Figure 1) even in 1 min (data is not shown). PFOS disappears in 2 h, while ~10% of residual F-53 was still detected during same period, requiring 3 hours in total for complete degradation. Hence, the observed degradation rate by UV/sulfite was F-53B > PFOS > F-53. This suggests that the presence of O atom in the perfluoroalkyl chain decreases the interaction of F-53 with hydrated electrons, as a result, slow down F-53 decomposition. On contrary, the fast degradation kinetics of F-53B indicates that the Cl atom accelerates the deconstruction of the molecule. In terms of defluorination, >90% of fluorine is recovered for F-53B, PFOS and F-53 after 8 h of reaction.

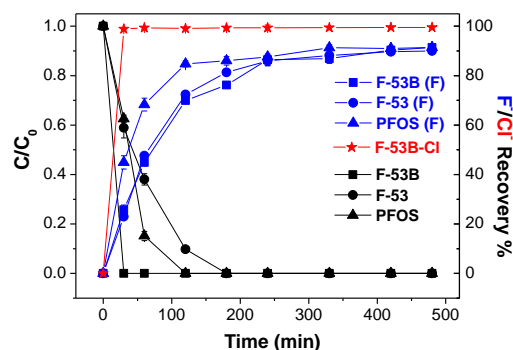


**Figure 1.** Degradation kinetics of F-53B, F-53 and PFOS; and fluoride/chloride ion recovery in UV/sulfite system ( $[\text{Na}_2\text{SO}_3] = 20$  mM, initial pH=10).

**Degradation of F-53B and PFOS in real electroplating effluent:** To assess the feasibility of UV/sulfite technique on treating F-53B and PFOS containing real industrial chrome plating wastewater. Effluent from electroplating streamline with 65.7  $\mu\text{g/L}$  of F-53B and 280.9  $\mu\text{g/L}$  of PFOS was employed for bench-scale experiment (Figure 2). More than 90% F-53B is degraded in wastewater after 30 min, and it is not detectable within 60 min. Comparing with F-53B degradation in ultrapure water (Figure 1), a dramatic decrease of reaction rate was observed. This was caused by other coexisting components in the wastewater, which would interfere with the  $e_{\text{aq}}^-$  attack. In contrast, only ~40% of PFOS was removed from effluent in 60 min, which implies that though UV/sulfite could be effective to degrade both PFOS and F-53B, the economical efficiency for PFOS would be quite low. Since sulfite is one of the most common reductant used to reduce Cr (VI) to Cr (III) in electroplating wastewater, the UV/sulfite could be a viable technology for removing F-53B in real electroplating effluent from both technical and economical point of views. Specifically, it is practical to integrate UV/sulfite technology into current effluent treatment processes just by adjusting sulfite dosage and introducing UV lights.

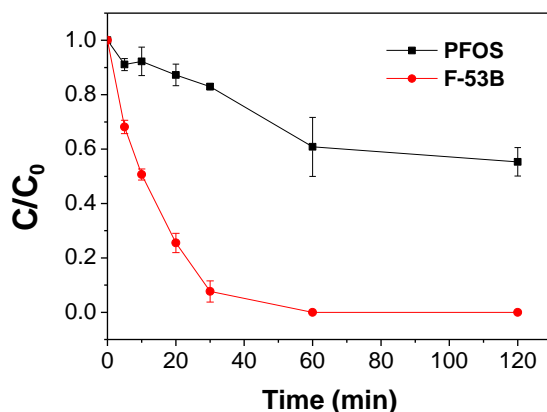


**Figure 2.** F-53B and PFOS degradation kinetics in real electroplating effluent by UV/sulfite ( $[\text{Na}_2\text{SO}_3] = 20 \text{ mM}$ , initial  $\text{pH}=10$ ).

**Degradation products of F-53B:** Concerning the degradation products of F-53B was not obtainable, some of them were qualitatively identified using scan mode according to the  $m/z$  values (Figure 3). A chromatogram peak is attributed to a hydrogen substituted F-53B ( $\text{HC}_6\text{F}_{12}\text{OC}_2\text{F}_4\text{SO}_3^-$ ,  $m/z = 496.9$ ) with a magnitude similar to that of F-53B ( $m/z = 530.9$ ). Therefore, dechlorination probably is one of the foremost reactions that lead to F-53B decomposition, as corroborated by the existence of the hydrogenated intermediate. Other intermediates are identified as  $\text{C}_6\text{O}_2\text{F}_{10}\text{Cl}^-$ ,  $m/z = 328.9$ ,  $\text{C}_6\text{HO}_2\text{F}_{10}^-$ ,  $m/z = 294.9$  and  $\text{C}_5\text{HO}_2\text{F}_8^-$ ,  $m/z = 244.9$ . When  $\text{Na}_2\text{SO}_3$  concentration is decreased to 2 mM, chlorides could not be complete recovered from solution. The intermediate with  $m/z = 328.9$  is actually corresponding to  $\text{ClC}_5\text{F}_{10}\text{COO}^-$ . The presence of such chlorinated intermediate suggests that F-53B is also split at ether bond.

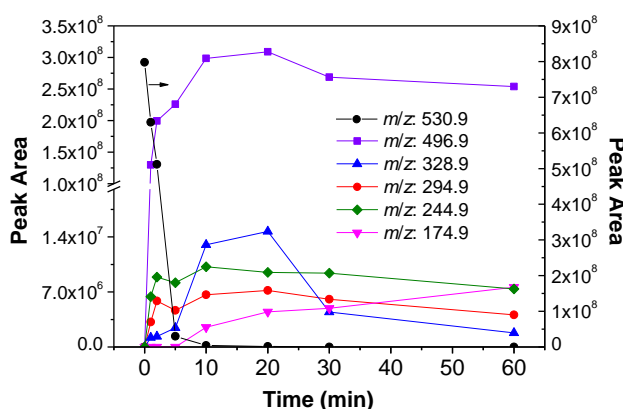


**Figure 3.** Variation of peak areas (average is adopted) of degradation products with respect to reaction time for F-53B by UV/sulfite ( $[\text{Na}_2\text{SO}_3] = 2 \text{ mM}$ ). (right Y-axis: F-53B ( $m/z$ : 530.9); left Y-axis: degradation products).

**Quantum chemistry calculation results:** The highest occupied molecular orbital (HOMO) contour surfaces of the investigated molecules (Figure 4a, c, e) indicate that, sulfonic acid group is the most reactive site for electrophilic attack. Yet, F-53B, F-53 and PFOS are not degradable by  $\text{SO}_4^{\cdot-}$  or  $\text{OH}^{\cdot}$  generated by UV/PS

system (data is not shown). In contrast, the lowest unoccupied molecular orbital (LUMO) contour surfaces of F-53, F-53B (Figure 4d, f) are changed by the insertion of O, or replacement of Cl to F, relative to LUMO of PFOS (Figure 4b). Comparing F-53 with PFOS, the total contribution of  $\alpha$ -carbon (C (8) in PFOS, C (9) in F-53) and  $\beta$ -carbon (C (7) in PFOS; C (8) in F-53) to LUMO decreases from 16.55% to 5.25%. This is more marked for the chlorinated congener (F-53B): the value decreases to 1.47% for F-53B. More importantly, contribution of F atoms on C (1) to LUMO of PFOS and F-53 are all negligible, while Cl contributes 21.58% to LUMO of F-53B. Besides, the substitution could also induce increase in the contribution of C (1) to LUMO for F-53B. From both experimental and quantum chemistry calculation results above, we think that the Cl atom determines significant enhancement of F-53B degradability in UV/sulfite system. To better understand such influence of O and Cl atom, vertical electron affinity (VEA, defined as the difference between total energies of a neutral molecular system and the anion in the same equilibrium geometry of the neutral system) were calculated. The VEA of PFOS is 109.1 kJ/mol, which is higher than that of F-53 (85.3 kJ/mol), but lower with respect to that of F-53B (132.2 kJ/mol). VEA fits well with degradation rate order, that is, F-53B > PFOS > F-53. It means that  $e_{aq}^-$  is more reactive toward F-53B rather than PFOS and F-53 in UV/sulfite system.

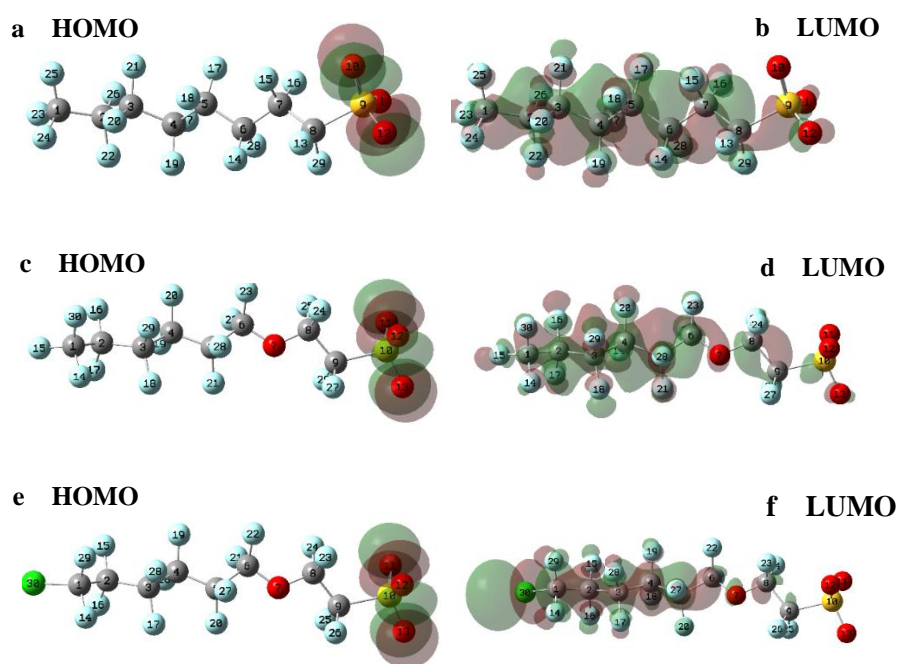


**Figure 4.** Contour surfaces of HOMO and LUMO of PFOS (a, b), F-53 (c, d) and F-53B (e, f), isovalue = 0.02.

**Degradation mechanisms and pathway of F-53B:** On the basis of experimental evidences and calculation results above, we propose a possible pathway for F-53B degradation (Figure 5). The pathway certainly starts with the attack of Cl atom in the F-53B molecule by  $e_{aq}^-$ . The identified intermediates, which can be divided in chloro-fluoro compounds and hydro-fluoro ones, suggest the existence of two possible types of reactions that could occur during the electron attack: hydrogenation (i.e. substitution of Cl by H with assisting of  $e_{aq}^-$ , named route I) and molecular cleavage (called route II). For initiation reaction of route I, Cl is replaced by H, thus resulting in generation of  $HC_6F_{12}OC_2F_4SO_3^-$  ( $m/z = 496.9$ ) (eq 1). Conceivably, this hydrogenated intermediated is then cleaved at the oxygen bridge (in Figure 4), forming  $\bullet OC_2F_4SO_3^-$  and  $HC_6F_{12}\bullet$ . As for route II, F-53B could be directly split at the O (7) by  $e_{aq}^-$  attack to give similar products to those from route I, apart from the presence of Cl replacement by H. Then, the two pathways of the perfluorinated fragment are similar: a continuous defluorination of the terminal carbon with unpaired electrons to generate the corresponding carboxyl acid<sup>8</sup>. The  $COO^-$  group then detaches from the molecular fragment,  $\bullet COO^-$  is likely transformed into  $CO_2$  (eq 2), but it also could react with other radicals ( $H\bullet$ ) to produce formic acid (eq 3)<sup>9</sup>. However, there were no formic acid detected in this system, maybe due to its low concentration. The  $\bullet OC_2F_4SO_3^-$  fragment, generated through both routes, probably reacts with water to form the alcohol. Similar to carboxylate generation, the sulfonated moiety may undergo stepwise defluorination to produce  $HOOC_2F_2SO_3^-$  ( $m/z = 174.9$ ). The described defluorination process is supposed to repeat itself until final delufluorination of all the intermediates of F-53B molecule. As for the observed defluorination rate is significantly slow and the fluoride recovery is not complete, it can be inferred that this cyclic pathway requires long reaction time.

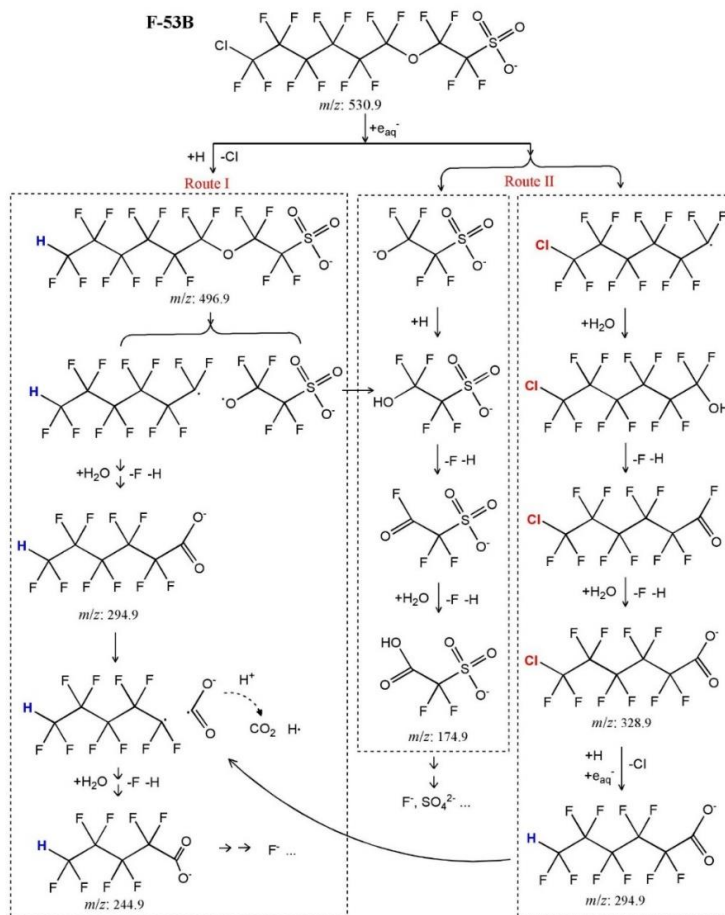
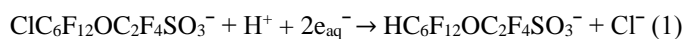


**Figure 5.** Possible degradation pathway of F-53B in UV/sulfite system.

F-53B is endowed with much better reducibility compared with PFOS due to the Cl atom replacement in the molecule. Consequently, its reducibility in real electroplating wastewater is greatly promoted relative to PFOS, and would make it more economical and efficient to remove F-53B from industrial effluent by integrating UV/sulfite process in current wastewater treatment units. As a potential alternative to PFOS, despite it is still oxidation-resistant, F-53B could be an ideal replacement for PFOS as CMS from reducibility perspective.

#### Acknowledgements:

We thank the financial support from Major Science and Technology Program for Water Pollution Control and Treatment in China (No. 2017ZX07202001 and 2017ZX07202004)

#### References:

1. Ti B, Li L, Liu J et al. (2018) *Sci. Total Environ.* 640-641: 1365-1371.
2. Shi G, Cui Q, Pan Y, et al. (2017) *Aquat Toxicol.* 185:67-75.
3. Shi Y, Vestergren R, Xu L, et al. (2016) *Environ. Sci. Technol.* 50(5): 2396-2404.
4. Cui Q, Pan Y, Zhang H, et al. (2018) *Environ. Sci. Technol.* 52(3): 982-990.
5. Zhang K, Cao Z, Huang J, et al. (2015) *Chem. Eng. J.* 286: 387-393.
6. Gao Y, Deng S, Du Z, et al. (2016) *J. Hazard. Mater.* 323 (Pt A): 550-557.
7. Chen H, Choi YJ, Lee LS, *Environ. Sci. Technol.* 52(17): 9827-9834.
8. Lee YC, Lo SL, Chiueh PT, et al. (2009) *Water Res.* 43(11): 2811-2816.
9. Qu Y, Zhang C, Li F, et al. (2010) *Water Res.* 44(9): 2939-2947.